Atomic and molecular collisions with surfaces: comparisons of Ar and N_2 scattering from Ru(0001)

2007 J. Phys.: Condens. Matter 19 305007

(http://iopscience.iop.org/0953-8984/19/30/305007)

IOP PUBLISHING JOURNAL OF PHYSICS: CONDENSED MATTER

J. Phys.: Condens. Matter **19** (2007) 305007 (15pp) doi:10.1088/0953-8984/19/30/305007

Atomic and molecular collisions with surfaces: comparisons of Ar and N_2 scattering from Ru(0001)

W W Hayes, Hailemariam Ambaye and J R Manson

Department of Physics and Astronomy, Clemson University, Clemson, SC 29634, USA

Received 5 February 2007, in final form 8 March 2007
Published 13 July 2007
Online at stacks.iop.org/JPhysCM/19/305007

Abstract

Recently reported molecular beam studies of Ar and N_2 scattering from Ru(0001) at thermal and hyperthermal energies exhibited a number of characteristics that are unusual in comparison to other systems for which molecular beam experiments have been carried out under similar conditions. For both systems the measured energy losses were unusually small. In the case of the Ar measurements some of the angular distributions exhibited an anomalous shoulder feature in addition to a broad peak near the specular direction, and quantum mechanical diffraction was observed under conditions for which it was not expected. These measurements are analysed and compared to calculations with a mixed quantum-classical scattering theory. This theory uses classical mechanics to describe the translational and rotational degrees of freedom while internal molecular vibrational modes are treated quantum mechanically. Many of the unusual features observed in the measurements are explained, but only upon using an effective surface mass of 2.3 Ru atomic masses, which implies collective effects in the Ru crystal. The large effective mass, because it leads to substantially larger Debye–Waller factors, explains and confirms the observations of diffraction features. It also leads to the interesting conclusion that Ru is a metal for which molecular beam scattering measurements in the purely quantum mechanical regime, where diffraction and single-phonon creation are dominant, should be possible not only with He atoms, but with many other atomic and molecular species with larger masses.

1. Introduction

Two different experimental groups have recently reported molecular beam measurements of scattering from clean, ordered Ru(0001) surfaces, using in one case atomic Ar atoms and in the other N_2 molecules as probes. Berenbak *et al* [1, 2] carried out an extensive experimental investigation of the Ru(0001) surface using scattering of beams of Ar atoms at thermal and hyperthermal energies, and as a part of an extensive study by the Odense group of N_2 interactions with the Ru(0001) surface Mortensen *et al* have reported detailed measurements for state-resolved inelastic scattering [3].

0953-8984/07/305007+15$30.00

Here, we review work in which these scattering data are compared to calculations using a theoretical model that has been useful in explaining surface collisions in other systems involving small atomic and molecular projectiles. This theory is a mixed classical-quantum treatment of surface scattering in which the translational and rotational degrees of freedom of the projectile are treated with classical mechanics while the excitation of internal molecular vibrational modes is treated quantum mechanically. The interaction potential is chosen to be a strongly repulsive barrier whose corrugation vibrates under the influence of the underlying target atoms.

Several unusual features were noted in the Ar/Ru(0001) scattered intensities, including smaller energy losses than predicted by simple analysis, and temperature-dependent broadening of the broad peaks observed in the energy-resolved spectra that deviated from the expected dependence, as well as observation of elastic diffraction peaks at lower incident energies. Quantum features such as diffraction peaks are not normally expected with such a large projectile mass and in the energy range investigated. The N_2/Ru(0001) experiments also measured smaller energy losses to the surface than expected.

Both sets of scattering data were originally analysed using the washboard model of Tully [4], and the Ar scattering was also analysed using a classical trajectory molecular dynamics simulation developed by Lahaye [5]. Neither of these two theoretical approaches was completely successful, at least for Ar scattering in the opinions of the authors of reference [1], because they gave only qualitative descriptions of the observed results.

A potentially important finding to come out of the comparisons is that, for both Ar and N_2 projectiles, in order to obtain agreement between theory and experiment it was necessary to choose an effective mass for the surface that was larger than that of a single Ru atom, whereas for most rare gas–metal systems a larger effective mass was not necessary. A larger effective mass can be interpreted as being due to collective phenomena in the metal in which the projectile scatters off an effective target of more than one substrate atom. Although analysis of molecular beam scattering from metals with the present theory usually gives satisfactory results using the mass of a single surface atom, there has been one other notable exception. This was a study of the rare gases Ne, Ar and Xe colliding with liquid Ga [6], in which the effective mass needed was 1.65 times the atomic gallium mass [7, 8]. Additional support for the idea of collective effects comes from the analysis of atomic and molecular scattering from Ru surfaces using the washboard model [4], which has also needed large effective masses [1, 3].

The manifestation of a larger effective mass for rare gases and molecules scattering from Ru surfaces has other implications aside from the fact that it indicates the presence of collective effects in this metal. It also implies that the Debye–Waller factors should be substantially larger than would be expected, since the exponential argument of the Debye–Waller factor in its simplest form is inversely proportional to the effective mass. Large Debye–Waller factors imply that quantum effects, such as diffraction and single surface phonon peaks, should be more readily observable for low incident energies. In fact, elastic diffraction was indeed observed in the Ar/Ru(0001) experiment [1], and has been also reported for argon scattering from hydrogen-terminated W(100) [9, 10] and for Ar scattering from Cu(111) for low temperatures and energies [11, 12]. An obvious conclusion from this observation is that, because of such a large effective surface mass, scattering at lower energies, such as used often in He atom scattering experiments, would lead to strong quantum mechanical features in the spectra. This implies that Ru is a metal for which molecular beam scattering measurements in the quantum mechanical regime, where diffraction and single-phonon creation are dominant, should be possible not just with light mass atoms, but also with other atomic and molecular projectiles with masses up to that of Ar atoms or even larger. The implication is that the dynamics of the electron density near

the surface of Ru can be probed by a large variety of neutral atomic and molecular projectiles through fully quantum mechanical measurements.

The organization of this paper is as follows: the next section gives a brief description of the theory, section 3 gives the results of the comparisons of calculations with the experimental data for Ar scattering, section 4 discusses the results for N_2 scattering, and in section 5 these comparisons are discussed and some conclusions are made.

2. Theory

For atom scattering at thermal and hyperthermal energies from metal surfaces, with the projectiles usually being the rare gases, the classical turning point of the interaction potential is at a substantial distance above the cores of the first layer of substrate atoms. The incoming projectiles scatter off a smoothly corrugated effective potential caused by Pauli repulsion between the overlap of the atomic electron cloud and surface electron density. The repulsive part of the interaction potential is roughly proportional to the surface electron density at the classical turning point, and the potential vibrates under the influence of the underlying substrate atoms [13]. A scattering theory that approximates this situation, and that has been successful in describing experimental observations of scattering from a number of systems, is the smooth surface model for which the incoming projectile collides with an otherwise flat surface, but one with thermal corrugations. It is expressed in terms of a differential reflection coefficient, $\mathrm{d}R\,(\mathbf{p}_\mathrm{f}, \mathbf{p}_\mathrm{i})/\mathrm{d}\Omega_\mathrm{f}\,\mathrm{d}E_\mathrm{f}^\mathrm{T}$, describing the probability of a particle with initial momentum $\mathbf{p}_\mathrm{i}$ being scattered into a small final translational energy $\mathrm{d}E_\mathrm{f}^\mathrm{T}$ and solid angle $\mathrm{d}\Omega_\mathrm{f}$ centred about the final momentum $\mathbf{p}_\mathrm{f}$. For a single collision it can be expressed in closed form, and is given by [14–16]

$$\frac{\mathrm{d}R\,(\mathbf{p}_\mathrm{f}, \mathbf{p}_\mathrm{i})}{\mathrm{d}\Omega_\mathrm{f}\,\mathrm{d}E_\mathrm{f}^\mathrm{T}} = \frac{m^2 v_\mathrm{R}^2 |\mathbf{p}_\mathrm{f}|}{8\pi^3 \hbar^2 p_{\mathrm{i}z} S_\mathrm{uc}} |\tau_\mathrm{fi}|^2 \left(\frac{\pi}{k_\mathrm{B} T_\mathrm{S} \Delta E_0^\mathrm{T}}\right)^{3/2} \exp\left\{-\frac{(E_\mathrm{f}^\mathrm{T} - E_\mathrm{i}^\mathrm{T} + \Delta E_0^\mathrm{T})^2 + 2v_\mathrm{R}^2 \mathbf{P}^2}{4k_\mathrm{B} T_\mathrm{S} \Delta E_0^\mathrm{T}}\right\}, \tag{1}$$

where $p_{\mathrm{i}z}$ is the surface-normal component of the incident momentum, k_B is Boltzmann's constant, m is the projectile atomic mass, $\Delta E_0^\mathrm{T} = (\mathbf{p}_\mathrm{f} - \mathbf{p}_\mathrm{i})^2/2M_\mathrm{C}$ is the recoil energy with M_C the target substrate mass, $\mathbf{P}$ is the parallel component of the scattering vector $\mathbf{p}_\mathrm{f} - \mathbf{p}_\mathrm{i}$, and $|\tau_\mathrm{fi}|^2$ is a form factor determined by the interaction potential. The factor S_uc is the area of a surface unit cell and v_R is a parameter having dimensions of speed that is explained in more detail below. Equation (1) can be derived from purely classical mechanics [15] or by starting from a quantum mechanical theory and taking the classical limit [14]. The quantum mechanical approach provides a means of determining the form factor $|\tau_\mathrm{fi}|^2$, and a good approximation is that τ_fi is the off-energy-shell transition matrix element of the elastic scattering potential [16, 17]. The quantum mechanical approach also identifies $\hbar$ as Planck's constant divided by 2π.

If the repulsive part of the interaction potential is flat and strongly repulsive, then the leading term in the perturbation series for the transition matrix element is

$$\tau_\mathrm{fi} = 4 p_{\mathrm{f}z}\, p_{\mathrm{i}z}/m, \tag{2}$$

a limiting form that has demonstrated its usefulness in previous studies of both atom and molecule scattering from surfaces.

The theory of equation (1) together with the form factor of equation (2) is what is used to carry out the calculations presented here for Ar/Ru(0001). Energy-resolved scattering spectra taken for fixed incident angle and beam energy and fixed final angles are compared directly to equation (1). Angular distributions for a fixed incident beam, which are the sum of all particles

scattered into the detector located at a specified final angle, are compared to

$$\frac{\mathrm{d}R}{\mathrm{d}\Omega_\mathrm{f}} = \int_0^\infty \mathrm{d}E_\mathrm{f}^\mathrm{T} \frac{\mathrm{d}R(\mathbf{p}_\mathrm{f}, \mathbf{p}_\mathrm{i})}{\mathrm{d}\Omega_\mathrm{f}\,\mathrm{d}E_\mathrm{f}^\mathrm{T}}. \tag{3}$$

The parameter v_R is completely determined by the phonon spectral density at the classical turning point [14]; thus its determination by comparison with experiment may provide useful information about the surface dynamics. However, it is usually treated as a parameter [14, 15], and crude estimates of its value give results of the order of the Rayleigh phonon velocity. For the Ar calculations presented here, the value of v_R is chosen to be 3200 m s^{-1}. This is to be compared with known measured values for the Rayleigh velocity of 3608 m s^{-1} for the Ru(0001) $\langle 11\bar{2}0\rangle$ direction and 3494 m s^{-1} for the $\langle 1\bar{1}00\rangle$ azimuth [18].

For the experimental data considered here, the incident Ar beam had a rather large energy spread, a roughly Gaussian-like distribution with a full width at half maximum of 0.042 eV [1]. This energy width has little effect on calculated angular distributions, since they are integrated over all final energies. However, a large energy width of the incident beam can have noticeable effects on the energy-resolved spectra. For the calculated results the differential reflection coefficient of equation (1) was convoluted with the experimentally measured energy distribution function [1].

For surface scattering of molecular beams the internal rotational and vibrational degrees of freedom must be included in the theory as well as the translational motion. Using theoretical approaches similar to those that produced equation (1), all three energy exchange channels can be included in the differential reflection coefficient. Taking the classical limits for translational and rotational motion, but retaining semiclassical quantum mechanics for the internal molecular vibrational modes, leads to the following general result for the differential reflection coefficient of a single collision [19–21]:

$$\begin{aligned}\frac{\mathrm{d}R(\mathbf{p}_\mathrm{f}, \mathbf{l}_\mathrm{f}; \mathbf{p}_\mathrm{i}, \mathbf{l}_\mathrm{i})}{\mathrm{d}\Omega_\mathrm{f}\mathrm{d}E_\mathrm{f}^\mathrm{T}} &= \frac{m^2|\mathbf{p}_\mathrm{f}|}{4\pi\hbar\, p_{\mathrm{i}z} S_\mathrm{uc}} |\tau_\mathrm{fi}|^2 \left(\frac{2\pi\hbar^2 v_\mathrm{R}^2}{\Delta E_0^\mathrm{T} k_\mathrm{B} T_\mathrm{S}}\right)\left(\frac{2\pi\hbar^2\omega_\mathrm{R}^2}{\Delta E_0^\mathrm{R} k_\mathrm{B} T_\mathrm{S}}\right)^{1/2} \\ &\times \left(\frac{\pi\hbar^2}{(\Delta E_0^\mathrm{T} + \Delta E_0^\mathrm{R}) k_\mathrm{B} T_\mathrm{S}}\right)^{1/2} \exp\left[-\frac{2\mathbf{P}^2 v_\mathrm{R}^2}{4\Delta E_0^\mathrm{T} k_\mathrm{B} T_\mathrm{S}}\right] \exp\left[-\frac{2l_z^2\omega_\mathrm{R}^2}{4\Delta E_0^\mathrm{R} k_\mathrm{B} T_\mathrm{S}}\right] \\ &\times \sum_{\kappa,\kappa'=1}^{N_\mathrm{A}} \left\{ \mathrm{e}^{\mathrm{i}(\mathbf{p}_\mathrm{f}\cdot\Delta\mathbf{r}_{\kappa,\kappa'}^f - \mathbf{p}_\mathrm{i}\cdot\Delta\mathbf{r}_{\kappa,\kappa'}^i)/\hbar}\, \mathrm{e}^{-W_\kappa(\mathbf{p}_\mathrm{f},\mathbf{p}_\mathrm{i})}\, \mathrm{e}^{-W_{\kappa'}(\mathbf{p}_\mathrm{f},\mathbf{p}_\mathrm{i})} \right. \\ &\times \prod_{j=1}^{N_v} \sum_{\alpha_j=-\infty}^{\infty} I_{|\alpha_j|}(b_{\kappa,\kappa'}(\omega_j)) \left[\frac{n(\omega_j)+1}{n(\omega_j)}\right]^{\alpha_j/2} \\ &\times \left. \exp\left[-\frac{(E_\mathrm{f}^\mathrm{T} - E_\mathrm{i}^\mathrm{T} + E_\mathrm{f}^\mathrm{R} - E_\mathrm{i}^\mathrm{R} + \Delta E_0^\mathrm{T} + \Delta E_0^\mathrm{R} + \hbar\sum_{s=1}^{N_v}\alpha_\mathrm{s}\omega_s)^2}{4(\Delta E_0^\mathrm{T} + \Delta E_0^\mathrm{R}) k_\mathrm{B} T_\mathrm{S}}\right] \right\}\end{aligned} \tag{4}$$

where $\mathbf{l}$ denotes angular momentum, N_A is the number of atoms in the projectile molecule, each denoted by index κ and mass m_κ, E^R is the rotational energy of the molecule, ω_R is a constant similar to v_R but for frustrated angular frequencies, $n(\omega_j)$ is the Bose–Einstein function for molecular vibrational frequency ω_j, $W_\kappa(\mathbf{p}_\mathrm{f}, \mathbf{p}_\mathrm{i})$ is the Debye–Waller exponent associated with internal mode excitation, and ΔE_0^R is the recoil energy for rotational motion. $I_{|\alpha_j|}(z)$ is the modified Bessel function of integer order α_j. The argument of the modified Bessel function of equation (4) is given by

$$b_{\kappa,\kappa'}(\omega_j) = \sum_{\beta,\beta'=1}^{3} p_\beta p_{\beta'} \frac{1}{N_v\hbar\sqrt{m_\kappa m_{\kappa'}}\,\omega_j}\, e(_j^\kappa|\beta)\, e^*(_j^{\kappa'}|\beta')\, \sqrt{n(\omega_j)[n(\omega_j)+1]}. \tag{5}$$

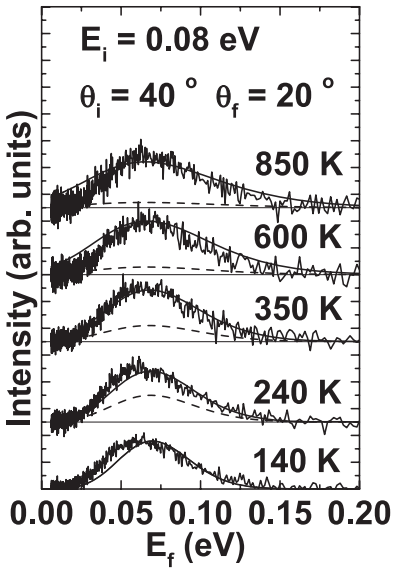

Figure 1. Energy-resolved spectra of Ar scattered from Ru(0001) at temperatures ranging from 140 to 850 K as marked. The incident energy is $E_\mathrm{i} = 0.08$ eV, the incident angle is $\theta_\mathrm{i} = 40°$, and the final angle is $\theta_\mathrm{f} = 20°$. The theoretical calculations, normalized to the data at each temperature, are shown as smooth solid curves and the calculated intensities relative to that at $T_\mathrm{S} = 140$ K are shown as dashed curves.

where $e(^{\kappa}_{j}|\beta)$ is the vibrational polarization vector for the jth internal mode and N_ν is the total number of such modes.

For compactness, the transition rate of equation (4) is expressed as a product over all normal modes labelled by j and a summation over the excitation quantum number denoted by α_j. The discrete state-to-state transition rate to a particular internal mode final state is obtained by taking the corresponding $(j,\ \alpha_j)$th term of equation (4). An expansion in terms of numbers of quanta excited in each of the internal modes can readily be carried out, and for many situations the single quantum terms are sufficient.

The differential reflection coefficients of equations (1) and (4) are used for the respective atomic and molecular calculations presented here.

3. Results: Ar scattering from Ru(0001)

A series of five measured energy-resolved intensity spectra as functions of final energy for argon scattering from Ru(0001) is shown in figure 1 for an incident energy $E_\mathrm{i} = 0.08$ eV, and incident polar angle $\theta_\mathrm{i} = 40°$, and with the detector positioned at the final angle $\theta_\mathrm{f} = 20°$. The surface temperatures range from $T_\mathrm{S} = 140$ to 850 K as marked. These spectra are characterized as smooth, broad, single-peaked structures which get broader with a longer high-energy tail at increasing temperature. The position of the peak, or most probable energy, remains essentially at the same position for all temperatures.

These energy-resolved spectra exhibit no evidence of quantum mechanical features such as sharp diffuse elastic or single surface phonon peaks. The expected classical nature under these conditions can be verified by evaluating the Debye–Waller factor $\exp\{-2W\}$, where the simplest approximation gives

$$2W = \frac{3(\mathbf{p}_f - \mathbf{p}_i)^2 T_S}{M_C k_B \Theta_D^2} = \frac{6\Delta E_0^T T_S}{k_B \Theta_D^2} \approx \frac{6m\left(\sqrt{E_i^T}\cos\theta_i + \sqrt{E_f^T}\cos\theta_f\right)^2 T_S}{M_C k_B \Theta_D^2}, \tag{6}$$

where the approximate evaluation is obtained by neglecting the parallel momentum transfer in favour of the much larger perpendicular momentum exchange. The exponent $2W$ is a measure of the approximate number of phonons created or destroyed in a collision, and when it is large the scattering is purely classical. Using for the surface mass M_C the mass of a single Ru atom and a value of 216 K for the Debye temperature [1] Θ_D, the value of $2W$ in the region of the most probable final energy is about 16 even at the lowest temperature. Such a large value would reduce all quantum features to negligible intensity, and indicate clear classical conditions.

Calculations from equation (1) are shown as solid lines, and for each temperature the calculations were normalized to the data at one point near the most probable intensity. The experimental data were reported in arbitrary units, and information about relative intensities at different temperatures was not determined. The theory of equation (1) predicts a decrease in the most probable intensity with T_S, and these relative theoretical calculations are shown as the dashed lines, normalized to the data at the lowest temperature of 140 K. The calculations match the general features of the data reasonably well; the increase in the high-energy tail is well predicted, but the calculations predict a larger increase of broadening with temperature than that observed.

However, as mentioned above, the calculations were carried out with an effective surface mass of 2.3 Ru atomic masses, a value that was determined by fitting the calculations to the experimental data of figure 1. The reason for this is that a smaller effective mass produces too much energy loss to the surface and gives curves that are too broad and do not match the most probable final energies observed in the data of figure 1. Without this larger effective mass, the calculated most probable final energy in figure 1 would be less than half that observed. The need for an effective mass is indicative of a collective effect in which several Ru atoms are involved in the collision process, and this is discussed further below in section 5. The value of the effective mass will also affect the Debye–Waller factor, implying that the value of $2W$ should be divided by 2.3. This would change the typical value calculated above to $2W \approx 7$ at the lower temperature and ranging up to over 30 at the higher temperatures, but these values are still large and within the range indicating classical scattering conditions.

It is of interest to examine the temperature dependence of the widths of the energy-resolved peaks of figure 1 because the theory of equation (1) predicts that the width should increase approximately as the square root of the temperature. These widths are shown in figure 2 which plots the squared full width at half maximum (FWHM) as a function of T_S. The data points taken from figure 1 are shown as open circles and the calculations are filled squares.

The square root dependence of the FWHM is obtained from equation (1) by making a Gaussian expansion of the argument about its minimum point. This gives the resulting approximations

$$(\mathrm{FWHM})^2 \approx 16\ln(2) g(\theta) E_i^T k_B T_S, \tag{7}$$

where $g(\theta)$ is a function of the mass ratio and total scattering angle θ [16].

It is seen that the theoretical points deviate from the Gaussian approximation of equation (7), exhibiting an increase with T_S that is less than expected. This behaviour is due to the convolution with the rather broad energy width of the experimental incident beam. Calculations assuming a monoenergetic incident beam have FWHMs that agree quite well with equation (7). The experimental data have widths that increase at a substantially slower rate with T_S than equation (7). The theoretical calculations in figure 2 indicate that part of this deviation may be due to the rather large energy definition of the incident beam. However,

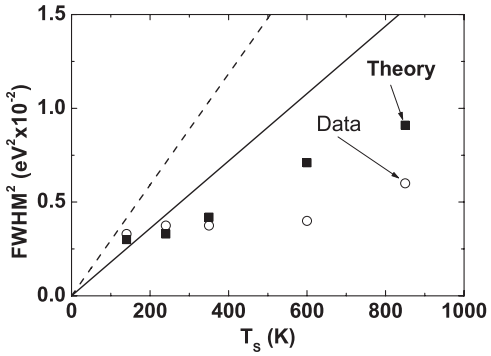

Figure 2. The squared FWHM plotted as a function of surface temperature T_S for the same data as shown in figure 1. Experimental points are shown as circles and calculations are shown as squares. The solid line is the Gaussian approximation to the present theory, and the dashed line is the result of the trajectory approximation.

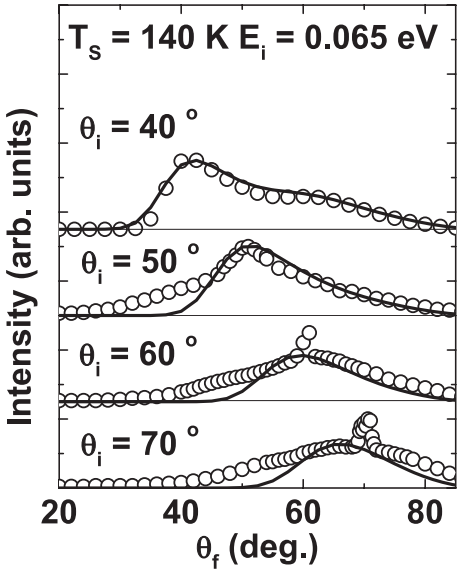

Figure 3. Angular distributions for Ar/Ru(0001)-(1 × 1)H in the $\langle 11\bar{2}0\rangle$ direction with E_i = 0.065 eV, T_S = 140 K and four different incident angles ranging from 40° to 70° as marked. The symbols are experimental data and the solid curves are calculations normalized to match the experimental data in the vicinity of the maximum in the background.

this temperature dependence of the data is unusual. In other experimental investigations of molecular beam scattering that have been compared with similar theoretical approaches as here, when the initial conditions indicated small Debye–Waller factors based on equation (6) and hence classical scattering conditions, the expected square-root dependence of the FWHM was quite well obeyed.

In addition to the results reported in [1], a number of scattering experiments were performed on a Ru(0001) surface with a (1 × 1) monolayer coverage of hydrogen atoms [2]. On this surface the azimuthal orientation was determined with low-energy electron diffraction (LEED) measurements, and in figure 3 are shown angular distributions taken with a low

incident energy of 0.065 eV, a surface temperature of 140 K and four incident angles from 40° to 70° separated by 10° intervals. At the most normal angle of $\theta_i = 40°$ the experimental points consist of a broad peak with a rather pronounced shoulder at about $\theta_f = 60°$, and for the more grazing incident angles a diffraction feature gradually appears at the specular position. For $\theta_i = 40°$ the value of $2W \approx 12$ at the specular position would seem to preclude the possibility of seeing a quantum peak, because even taking into account the effective mass would reduce this to about 5, which is still a rather large value for observing quantum effects. However, at the larger, more grazing angles the $2W$ value becomes smaller, and for $\theta_i = 70°$, where $2W \approx 3$ (evaluated with the effective mass of a single Ru atom), a distinct specular diffraction peak is observed.

The calculations shown as solid curves in figure 3 were carried out assuming a clean Ru(0001) surface, i.e., ignoring the adsorbed H atoms. There is little reason to suspect that the tightly bound hydrogen overlayer would have a noticeable effect on the scattering of a heavy projectile such as Ar. However, this question was directly addressed by some of the authors of [1] in a series of experiments in which Ar scattering measurements from clean and (1×1) hydrogen-covered Ru(0001) were compared directly under otherwise identical initial conditions. No detectable differences in the scattered spectra were observed as a result of the hydrogen adsorbates [22].

At the angle closest to normal $\theta_i = 40°$ in figure 3, where the Debye–Waller evaluation clearly indicates classical scattering conditions, the calculations agree very well with the data, and this agreement includes the interesting shoulder feature. At the more grazing angles, since the exponent $2W$ near the specular position varies approximately as $\cos^2\theta_i$, the Debye–Waller factor increases quickly, allowing the specular quantum diffraction to appear. In fact, if the effective mass is used $2W$ becomes ≈ 1 at the largest angle of 70°, making this case clearly in the quantum regime. For these larger angles where quantum effects are important, the present classical mechanical calculations are not expected to be valid, and they explain only qualitatively the broad background under the specular peak.

The good agreement for the clearly classical scattering conditions for $\theta_i = 40°$ is quite interesting. In the calculations, the reason for the shoulder appearing in the neighbourhood of $\theta_f = 60°$ is due to the nature of the differential reflection coefficient of equation (1). Its important features are two Gaussian-like functions, one in the energy transfer $E_f^T - E_i^T - \Delta E_0^T$ and the other in the parallel momentum transfer $\mathbf{P}$. Although the angular distribution consists of an integral over all final energies, the dominant contribution to this integral comes from the region of final energies in the neighbourhood of the minima of the argument of the exponential appearing in equation (1). Typically, this results in a scattered angular distribution that has a single broad peak in the general neighbourhood of the specular position. For given incident and final angles, the argument of the exponential in equation (1) does not necessarily vanish, because this would require the simultaneous conditions $E_f^T - E_i^T - \Delta E_0^T = 0$ and $\mathbf{P} = 0$. However, the shoulder at $\theta_f \approx 60°$ appearing in figure 3 can be associated with conditions in which these simultaneous requirements are satisfied, i.e., conditions in which the minimum of the argument of the exponential actually is zero. In order to understand this better, it is of interest to consider each of the two Gaussian-like functions separately. In the range of final energies $0 < E_f^T < \infty$ the condition $E_f^T - E_i^T - \Delta E_0^T = 0$ is always satisfied if the mass ratio $m/M_C < 1$ for any combination of incident and final angles. (For the case $m/M_C > 1$ the situation becomes more complicated, but this is not of interest for the present Ar/Ru system.) The condition $\mathbf{P} = 0$ is usually not simultaneously satisfied. However, under certain special circumstances both may be simultaneously satisfied. One of these circumstances is when θ_i is near normal and θ_f is larger and there is net energy loss to the surface, precisely the conditions of figure 3. The condition $E_f^T - E_i^T - \Delta E_0^T = 0$ requires $E_f^T < E_i^T$, and the in-plane parallel

momentum transfer which is proportional to $\sqrt{E_i^T}\sin\theta_i - \sqrt{E_f^T}\sin\theta_f$ can also simultaneously vanish because $\sin\theta_f > \sin\theta_i$, and in fact this may occur at more than one angle.

Thus, it is the vanishing of the argument of the exponential of equation (1) that causes the broad and unexpectedly intense shoulder at large supraspecular angles in figure 3. Its intensity is dependent on the effective mass and temperature. The shoulder is distinctly less prominent if M_C equals a single Ru atomic mass and becomes increasingly apparent with larger M_C. As T_S increases it disappears. Since the Gaussian-like function in **P** that causes this shoulder arises from the fundamental condition of parallel momentum conservation in phonon transfer, and since it can be related to vibrational correlations between closely neighbouring positions on the surface, this feature is surely worthy of further investigation. Potentially, even more direct and important information should be obtained from measurements of the energy-resolved spectra for this case, as is discussed further in section 5 below.

4. Results: N_2 scattering from Ru(0001)

The Odense group has carried out a large number of experiments on various aspects of N_2 interactions with the Ru(0001) surface, among them investigations of adsorption, desorption, sticking and chemical reactions [23, 24]. This series of investigations has also produced detailed measurements for state-resolved inelastic scattering [3]. The N_2/Ru(0001) system is of very active current interest in ongoing debates concerning the applicability of the Born–Oppenheimer approximation in the interaction of molecules with metal surfaces. Calculations of N_2 dissociation based on density functional theory predict very efficient energy loss to electronic excitations in Ru(0001) [25], while classical trajectory calculations indicate that multidimensional effects associated with translational and rotational motion are much more important than nonadiabatic effects [26].

The most important and accurate measurements made were for the average final translational energy normal to the surface $\langle E_{fn}^T\rangle$ as a function of final rotational energy E_f^R. These are shown in figure 4(a) for two different energies and incident beam angles, $E_i^T = 1.5$ eV with $\theta_i = 19°$ and $E_i^T = 2.4$ eV with $\theta_i = 0°$, and the surface temperature is 610 K for all data shown. These are compared with two sets of calculations, one using the mass of Ru as the surface mass and the other with an effective surface mass 2.3 times that of a single Ru atom [27]. For all calculations for N_2 the value of the velocity parameter v_R is 1000 m s^{-1}, while the frequency parameter ω_R is given a value so small it has no effect on the calculations. Only qualitative agreement with the negative correlation between $\langle E_{fn}^T\rangle$ and E_f^R is obtained using the smaller mass. However, with the larger effective surface mass quantitative agreement is obtained, and this holds true for essentially all of the comparisons presented here. The implication is that N_2 scattering from Ru(0001) results in much smaller translational energy transfers to the surface than would be predicted from simple models of collisions between N_2 and an isolated Ru atom.

Figure 4(b) shows a different way of presenting the negative correlation of figure 4(a) that includes the effects of energy transfer to the other degrees of freedom of the scattered molecules. Plotted in figure 4(b) as a function of E_f^R is the quantity $\langle\Delta E_s\rangle = E_{in} - \langle E_{fn}^T\rangle - \langle\Delta E_\parallel^T\rangle - \langle\Delta E^R\rangle - \langle\Delta E_v\rangle$, the fractional normal incident energy lost to all degrees of freedom. The quantities $\langle\Delta E_\parallel^T\rangle$, $\langle\Delta E^R\rangle$, and $\langle\Delta E_v\rangle$ are the average transfer of energy to parallel translational, rotational, and vibrational degrees of freedom, respectively. Again, the calculations with the larger effective surface mass give reasonable quantitative agreement with experiment. In the calculations $\langle\Delta E_v\rangle$ was negligible, in agreement with experimental observations. It should be noted that reference [3] also reported two data points taken at

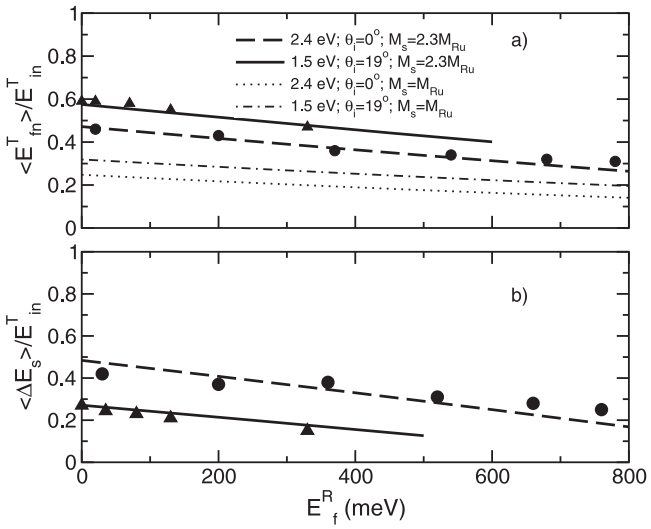

Figure 4. (a) The average normal translational energy $\langle E_{\rm fn}^{\rm T}\rangle/E_{\rm in}^{\rm T}$ as a function of final rotational energy $E_{\rm f}^{\rm R}$. (b) Average fractional energy loss to the surface $\langle\Delta E_{\rm s}\rangle/E_{\rm in}^{\rm T}$ versus $E_{\rm f}^{\rm R}$. Incident beam conditions are $E_{\rm i} = 2.4$ eV and $\theta_{\rm i} = 0°$ with data shown as circles and $E_{\rm i} = 1.5$ eV and $\theta_{\rm i} = 19°$ shown as triangles.

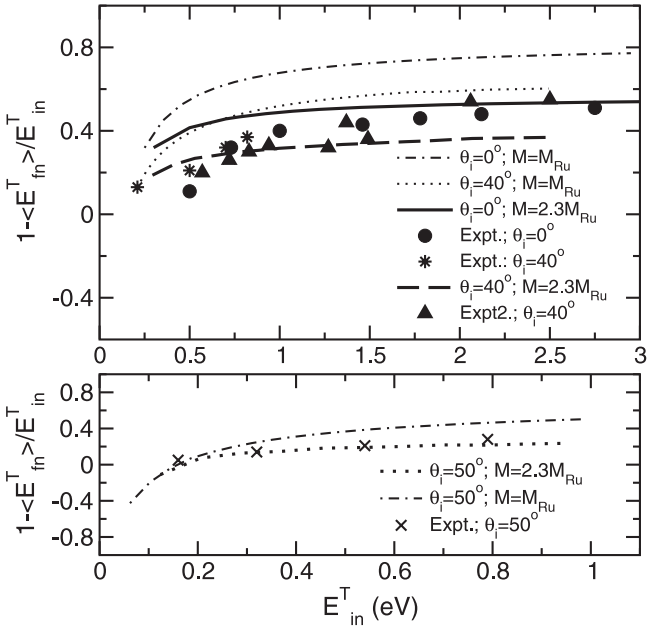

Figure 5. The normal translational energy loss as a function of the normal incident energy $E_{\rm in}$. The top panel is for $\theta_{\rm i} = 40°$ and $\theta_{\rm i} = 0°$ and the bottom panel is for $\theta_{\rm i} = 50°$.

$E_{\rm i}^{\rm T} = 2.7$ eV and $\theta_{\rm i} = 19°$ with which our calculations also agree, but for clarity these are not shown.

The incident energy dependence of the average final translational energy is shown in figure 5, where the normalized energy difference $1 - \langle E_{\rm fn}^{\rm T}\rangle/E_{\rm in}^{\rm T}$ is plotted for several incident

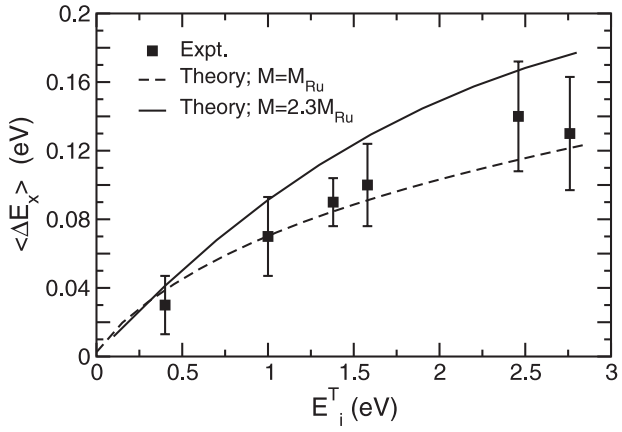

Figure 6. The average energy change $\langle \Delta E_x^{\mathrm{T}} \rangle$ associated with the transfer of momentum perpendicular to the plane of scattering.

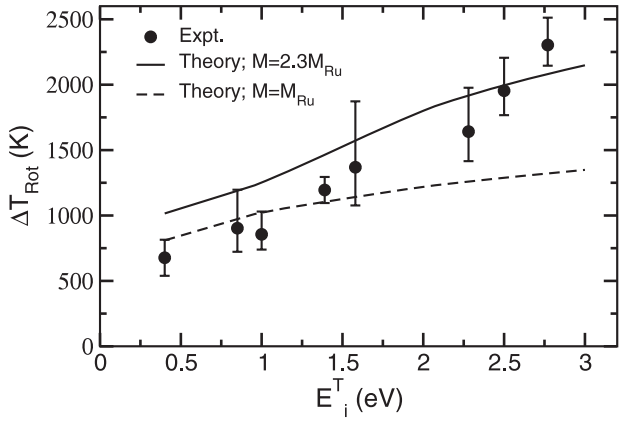

Figure 7. The difference between the final and initial rotational temperature ΔT_{rot} as a function of the incident translational energy E_{i}.

beam angles as marked. The data for $\theta_{\mathrm{i}} = 40°$ denoted by asterisks and those at $\theta_{\mathrm{i}} = 50°$ denoted by $(\times)$ symbols were extracted from [28] by the authors of reference [3]. Calculations are shown for the two masses, and reasonable agreement is obtained with the $\theta_{\mathrm{i}} = 50°$ data for the higher mass. The data at angles other than 50° are only qualitatively explained, but the better agreement is with the larger effective surface mass.

The average energy transfer perpendicular to the plane of scattering $\langle \Delta E_x^{\mathrm{T}} \rangle$ is shown in figure 6 as a function of incident energy E_{i} with an incident angle $\theta_{\mathrm{i}} = 19°$. The calculations for the larger surface mass show the biggest out-of-plane energy transfers for incident energies greater than 0.4 meV, as expected since a larger surface mass leads to less overall energy transfer and hence higher translational energy in all directions of scattered particles. In this case, however, it is significant that the better overall agreement with experiment is for an effective mass equal to that of one Ru atom.

Rotational temperatures of the scattered spectra as functions of incident energy are compared with the calculated predictions in figure 7, and again better quantitative agreement is obtained with a larger effective mass.

Reasonable agreement of the present theory with observations is obtained, but with the exception of parallel energy transfer out of the scattering plane, only when a larger effective mass is used for the Ru surface. The collective effect, implied by a larger effective mass, has been noted in other attempts using simpler models to compare calculations with molecular scattering measurements from Ru surfaces [22]. For molecular scattering from other metal surfaces a larger effective mass has not been necessary using present theoretical methods [19–21, 29]. The fact that a larger effective mass is not needed for the case of energy transfer in directions parallel to the surface is suggestive that the collective effect involves Ru atoms in layers below the surface, and not parallel to the surface.

5. Discussion and conclusions

A classical theory of atomic collisions with surfaces has been used to analyse and compare newly available experimental data for the scattered intensities produced by beams of Ar atoms and N_2 molecules directed towards a Ru(0001) surface. The present theoretical analysis, using a calculational model that has proved to be useful in explaining atomic and molecular beam scattering under classical conditions for a number of other systems, appears to resolve the question of why diffraction peaks are so readily visible in the Ar/Ru(0001) system. The observed energy-resolved spectra and angular distributions for both Ar and N_2 projectiles can be explained only if they are assumed to be scattering from a collection of more than one Ru atom which has an effective mass of approximately 2.3 Ru atomic masses.

This collective effect is most readily seen in the energy-resolved spectra shown in figure 1, or in the final normal energies measured for N_2 shown in figure 4. The calculations exhibit energy losses which are far too large if one assumes that the surface mass is that of a single Ru atom. However, with a mass $M_C = 2.3$ Ru atoms the agreement with the theory is in reasonable agreement with the measurements.

This answers the question of why quantum diffraction effects could be observed in the Ar experiments. The same effective mass is what appears in the denominator of the Debye–Waller exponent $2W$ of equation (6), which implies that $2W$ is actually $1/2.3$ times smaller, and consequently the Debye–Waller factor much larger, allowing quantum effects to be readily seen under conditions of small incident energies and low surface temperatures.

It is important that the same effective mass was detected by two projectiles of widely different physical properties. The present analysis provides confirmation that the collective effect is due to the Ru surface and is not an effect of the nature of the projectile. The N_2/Ru(0001) scattering experiment was also able to independently measure average energies of the final distributions corresponding to motion parallel and perpendicular to the surface as shown in figure 6. Analysis of this indicated that the collective effect was with Ru atoms in layers beneath the surface and not with neighbouring atoms in the surface layer.

This observation of collective effects leads to an interesting prediction. The unusual nature of the Ru surface, with its large effective mass for atomic and molecular scattering, means that Ar atoms at subthermal energies, energies that are known to be readily achievable in He scattering experiments [30], can be used for scattering investigations in the purely quantum mechanical regime. This would, by extension, also imply that other atomic and molecular projectiles, and at least those with masses intermediate between hydrogen and argon, should also scatter very quantum mechanically. Thus, ruthenium appears to present a somewhat unique system in which surface structure and dynamics could be studied by quantum mechanical scattering of a large range of quite different atomic and molecular probes.

The temperature dependence of the energy-resolved spectra for Ar scattering from Ru(0001) was also anomalous in comparison to virtually all other atomic and molecular

surface systems that have been measured under classical scattering conditions. Theories such as that of equation (1) show that the FWHM should increase with the square root of the surface temperature, as in equation (7), and this is a consequence of the fundamental condition of equipartition of energy. The present experiments exhibit an FWHM that increases with temperature, but substantially less strongly than expected, as shown in figure 2. The present analysis shows that at least some of this anomalous behaviour is due to the very large energy spread of the incident beam at low energies, because when the differential reflection coefficient of equation (1) is convoluted with the experimental energy distribution the calculated FWHMs also have a less strong increase with T_S.

One of the Ar angular distribution measurements exhibited a highly unusual shoulder at supraspecular angles, and this was the case of the hydrogen-covered Ru(0001) shown in figure 3 for which the surface temperature was low (140 K) and the incident energy was small (0.065 eV). For $\theta_i = 40°$, the scattering conditions, even taking into account the larger effective mass, were well into the classical multiphonon regime, as confirmed by evaluation of the Debye–Waller factor. The observed angular distribution was a very broad function of final angle, with a broad peak at the specular position and a second broad shoulder-like feature in the neighbourhood of $\theta_f = 60°$. The calculations reproduced this shoulder feature very nicely. In the theory, both features could be identified as being caused by the double-Gaussian-like nature of the differential reflection coefficient (1). The broad specular peak occurs because the differential reflection coefficient of equation (1) tends to have its maximum values in this region. The shoulder is caused by a special combination of small incident angle and large final angle that allows the argument of the Gaussian-like function in equation (1) to vanish, giving rise to another region where local maxima in the differential reflection coefficient occur.

This explanation of the shoulder appearing in figure 3 leads immediately to suggestions for interesting further experiments. More detailed experiments, particularly energy-resolved experiments for final angles near specular and near the position of the shoulder, should be able to separate out the effects of the two Gaussian-like terms in the differential reflection coefficient [31]. This should provide a more precise value of the parameter v_R which, in turn, will provide physical information on the correlations of the surface electron density at nearby separations.

The reasoning behind the preceding statement is as follows: the quantity v_R, which appears in both the atomic and molecular scattering theories of equations (1) and (4), is actually a well-defined weighted average of all phonon velocities parallel to the surface [14]. It arises because of the fundamental condition of conservation of momentum parallel to the surface for each of the many phonons transferred. Because, in a classical scattering event, many phonons are generated, this translates into the Gaussian-like function in parallel momentum transfer **P** appearing in equations (1) and (4). This Gaussian-like function is a correlation function, and its Fourier transform, which is a Gaussian-like correlation function in positions parallel to the surface, provides an effective length R_C over which the collision process samples the correlations of the surface. If the Gaussian-like function in equation (1) is expressed in terms of this correlation length according to

$$\exp\left\{-\frac{2v_R^2\mathbf{P}^2}{4k_B T_S \Delta E_0}\right\} = \exp\left\{-\frac{\mathbf{P}^2 R_C^2}{\hbar^2}\right\}, \tag{8}$$

the temperature and energy dependence of R_C can be evaluated in terms of the Debye–Waller exponent of equation (6), and for the present Ar/Ru system the result is $R_C = 1.9/\sqrt{2W}$ Å.

Thus, precise measurements of v_R, and its dependence on the scattering parameters, can lead to important new physical information on the surface dynamics and correlation, and the unusual shoulder feature of the angular distribution of figure 3 seems to provide a very

interesting case for further examination. Since the repulsive part of the interaction potential is, to a good approximation, directly proportional to the surface electron density at the classical turning point, this implies that knowledge of v_R can be related to vibrational correlations in the surface electron density at distances of order R_C.

To conclude, it is of interest to reiterate the interesting and anomalous features observed in these molecular beam scattering experiments, to review the information that the present theoretical analysis is able to provide, and to make some suggestions for interesting new experiments. The measurements exhibit the following characteristics that are unusual in comparison to other systems that have been investigated under similar conditions: (1) the energy losses exhibited in the energy-resolved measurements are surprisingly small, (2) the temperature-dependent increase in FWHM of the energy-resolved spectra is weaker than predicted, (3) many of the angular distributions exhibit narrower peaks than expected, (4) some of the angular distributions exhibited an anomalous shoulder feature in addition to a peak near the specular position, and (5) quantum mechanical diffraction was observed under conditions for which it was not expected.

These points are explained, at least qualitatively to some degree, by the present theoretical analysis. All of these features point towards a collective effect in the Ru crystal that results in an effective mass for the collision of $\approx$2.3 atomic masses of Ru, an effective mass that is independent of projectile.

The N_2 experiments provided some limited evidence that the collective effect was with Ru atoms in crystal layers below the surface, and not with the in-plane atoms in the outermost surface layer. Additional experiments could clarify the role of Ru atoms in the surface layer versus those in deeper layers if they are carried out for conditions that distinguish the transfer of parallel and perpendicular momentum. What is needed in order to answer this question are energy-resolved measurements under conditions where the transfer of momentum is nearly perpendicular, which implies near-normal incident and final angles, contrasted with measurements taken under conditions that favour parallel momentum transfer, which implies that at least one of the incident or final angles should be at a near-surface-grazing position. Also helpful would be experiments from which average energies associated with motion parallel and perpendicular to the surface could be measured.

The anomalous shoulder observed in the Ar angular distributions for the Ru(0001)-(1×1)H surface shown in figure 3 also provides interesting suggestions for new experimental investigations. Detailed measurements of energy-resolved spectra for this case have the potential for revealing information about vibrational correlations of the surface electron density at short distances.

Perhaps the most important observation to come out of this work is the fact that the present calculations support and confirm the observation of quantum mechanical diffraction features in the experiments. On the basis of assuming a surface mass of a single Ru atom, quantum effects would be predicted to be unobservable under experimental conditions in which they definitely were observed. It is now obvious, however, because the present calculations show clearly that the effective mass is that of about 2.3 Ru atoms, that diffraction and other quantum effects are not only observable but are to be expected for scattering under a broad range of incident conditions at low energies. This leads to the interesting conclusion that Ru is a metal for which scattering experiments in the purely quantum regime could be readily carried out with a wide range of atomic and molecular probes. Because of their widely differing masses and electronic properties, quantum diffraction and single-phonon measurements with a variety of projectiles would provide interesting comparative structural and dynamical information on the surface electron density at different classical turning point distances from the outermost surface layer. For example, a comparative examination of both He and Ne atom diffraction from

hydrogen-covered nickel and rhodium surfaces was able to demonstrate clear anticorrugating effects due to the differences in hybridization of the orbitals of the two incoming atoms with the unoccupied metal states [32]. The availability of different quantum mechanical projectiles with a range of masses and electronic distributions for probing Ru surfaces could lead to similar important comparative studies on this system.

Acknowledgments

We would like to thank B Berenbak and A W Kleyn helpful discussions on the Ar/Ru(0001) system and for making their data available to us. We would like to thank Alan Luntz for helpful discussions on the scattering of N_2 from Ru(0001). This work was supported by the US Department of Energy under grant number DE-FG02-98ER45704.

References

[1] Berenbak B, Zboray S, Riedmuller B, Papageorgopoulos D C, Stolte S and Kleyn A W 2002 *Phys. Chem. Chem. Phys.* **4** 68
[2] Berenbak B 2000 *PhD Thesis* Vrije Universiteit Amsterdam, The Netherlands , unpublished
[3] Mortensen H, Jensen E, Diekhöner L, Baurichter A, Luntz A C and Petrunin V V 2003 *J. Chem. Phys.* **118** 11200 (a review of other N_2 surface interaction papers is given here)
[4] Tully J C 1990 *J. Chem. Phys.* **92** 680
[5] Lahaye R J W E 1995 *PhD Thesis* Vrije Universiteit Amsterdam, The Netherlands, unpublished
[6] Manning M, Morgan J, Castro D and Nathanson G M 2003 *J. Chem. Phys.* **119** 12593
[7] Muis A and Manson J R 1997 *J. Chem. Phys.* **107** 1655
[8] Hayes W W and Manson J R 2007 to be published
[9] Schweizer E K and Rettner C T 1989 *Phys. Rev. Lett.* **62** 3085
[10] Schweizer E K, Rettner C T and Holloway S 1991 *Surf. Sci.* **249** 335
[11] Althoff F, Andersson T and Andersson S 1997 *Phys. Rev. Lett.* **79** 4429
[12] Šiber A and Gumhalter B 1998 *Phys. Rev. Lett.* **81** 1742
[13] Celli V 1992 *Helium Atom Scattering* (*Springer Series in Surface Sciences* vol 27) ed E Hulpke (Heidelberg: Springer) p 25
[14] Brako R and Newns D M 1982 *Phys. Rev. Lett.* **48** 1859
Brako R 1982 *Surf. Sci.* **123** 439
[15] Meyer H-D and Levine R D 1984 *Chem. Phys.* **85** 189
[16] Manson J R 1991 *Phys. Rev.* B **43** 6924
[17] Manson J R 1994 *Comput. Phys. Commun.* **80** 145
[18] Braun J, Kostov K L, Witte G, Surnev L, Skofronick J G, Safron S A and Wöll Ch 1997 *Surf. Sci.* **372** 132
[19] Iftimia I and Manson J R 2001 *Phys. Rev. Lett.* **87** 093201
Iftimia I and Manson J R 2002 *Phys. Rev.* B **65** 125412
[20] Ambaye H, Manson J R, Weiße O, Wesenberg C, Binetti M and Hasselbrink E 2004 *J. Chem. Phys.* **121** 1901
[21] Ambaye H and Manson J R 2006 *J. Chem. Phys.* **125** 084717
[22] Riedmüller B, Ciobîcă I M, Papageorgopoulos D C, Berenbak B, van Santen R A and Kleyn A W 2000 *Surf. Sci.* **465** 347
[23] Diekhöner L, Hornekaer L, Mortensen H, Jensen E, Baurichter A, Petrunin V V and Luntz A C 2002 *J. Chem. Phys.* **117** 5018
[24] Diekhöner L, Mortensen H, Baurichter A, Jensen E, Petrunin V V and Luntz A C 2001 *J. Chem. Phys.* **115** 9028
[25] Luntz A C and Persson M 2005 *J. Chem. Phys.* **123** 074704
[26] Dáz C, Vincent J K, Krishnamohan G P, Olsen R A, Kroes G J, Honkala K and Nørskov J K 2006 *Phys. Rev. Lett.* **96** 096102
[27] Ambaye H and Manson J R 2006 *J. Chem. Phys.* **125** 176101
[28] Papageorgopoulos D C, Berenbak B, Verwoest M, Riedmüller B, Stolte S and Kleyn A W 1999 *Chem. Phys. Lett.* **305** 401
[29] Moroz I and Manson J R 2005 *Phys. Rev.* B **71** 113405
[30] A collection of review articles on He atom scattering appears in: Hulpke E (ed) 1992 *Helium Atom Scattering* (*Springer Series in Surface Sciences* vol 27) (Heidelberg: Springer)
[31] Hayes W W and Manson J R 2006 *Phys. Rev.* B **74** 073413
[32] Rieder K H, Parschau G and Burg B 1993 *Phys. Rev. Lett.* **71** 1059

J. Phys.: Condens. Matter **20** (2008) 219801 (1pp) doi:10.1088/0953-8984/20/21/219801

Erratum

Atomic and molecular collisions with surfaces: comparisons of Ar and N_2 scattering from Ru(0001)
W W Hayes, Hailemariam Ambaye and J R Manson
J. Phys.: Condens. Matter **19** 305007

Due to an error in the calculations, figures 1–3 are incorrect. The corrected figures are shown below. The discussion of figure 1 is unchanged. However, our disussion of figure 2 with respect to the effects of convolution with the energy width of the experimental incident beam are no longer valid. The calculated points in figure 2 now agree reasonably well with the Gaussian approximation of equation (7) except for the point at the highest surface temperature where the Gaussian approximation begins to break down. In the discussion of figure 3 the considerations of the shoulder feature for $\theta_i = 40^\circ$ at $\theta_f \approx 60^\circ$ no longer apply. The corrections do not change the conclusions of the paper regarding evidence for an effective mass larger than that of a single Ru atom and all conclusions drawn from this finding remain valid.

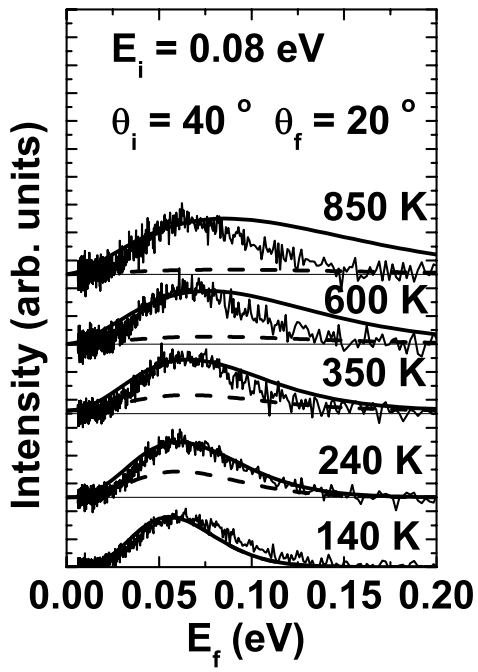

Figure 1. Energy resolved spectra of Ar scattered from Ru(0001) at temperatures ranging from 140 to 850 K as marked. The incident energy is $E_i = 0.08$ eV, the incident angle is $\theta_i = 40^\circ$, and the final angle is $\theta_f = 20^\circ$. The theoretical calculations, normalized to the data at each temperature, are shown as smooth solid curves and the calculated intensities relative to that at $T_S = 140$ K are shown as dashed curves.

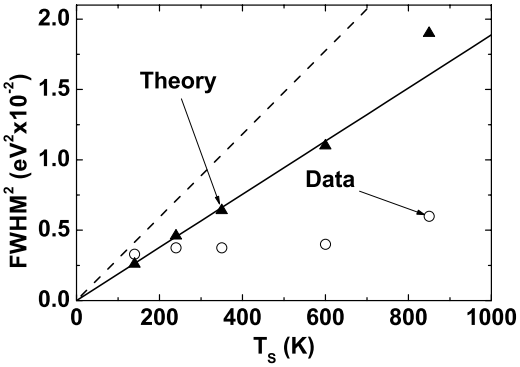

Figure 2. The squared FWHM plotted as a function of surface temperature T_S for the same data as shown in figure 1. Experimental points are shown as circles and calculations are shown as squares. The solid line is the Gaussian approximation to the present theory, and the dashed line is the result of the trajectory approximation.

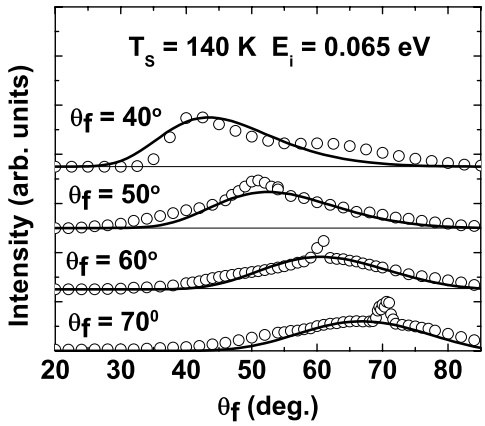

Figure 3. Angular distributions for Ar/Ru(0001)-(1×1)H in the $\langle 11\bar{2}0 \rangle$ direction with $E_i = 0.065$ eV, $T_S = 140$ K and four different incident angles ranging from 40° to 70° as marked. The symbols are experimental data and the solid curves are calculations that have been renormalized to match the experimental data in the vicinity of the maximum in the background.

